J. Phycol. **57,** 975–987 (2021)

DOI: 10.1111/jpy.13140-20-267

THALLUS GROWTH STAGE AND GEOGRAPHIC ORIGIN SHAPE MICROALGAL DIVERSITY IN *RAMALINA FARINACEA* LICHEN HOLOBIONTS[1]

Arantzazu Molins,[2,*] *Patricia Moya*[*]

Instituto "Cavanilles" de Biodiversidad y Biología Evolutiva, Botánica, Fac. CC. Biológicas, Universitat de València, 46100 Burjassot, Valencia,Spain

Lucia Muggia

Department of Life Sciences, University of Trieste, via L. Giorgieri 10,34127 Trieste, Italy

and Eva Barreno

Instituto "Cavanilles" de Biodiversidad y Biología Evolutiva, Botánica, Fac. CC. Biológicas, Universitat de València, 46100 Burjassot, Valencia,Spain

Lichen symbioses are microecosystems hosting many other living organisms besides the two major lichen symbionts (i.e., lichenized fungi [the mycobiont] and green microalgae or cyanobacteria [the photobiont]). Recent investigations evidenced that other fungi, non-photosynthetic bacteria, and microalgae co-inhabit within the lichen thalli, but their diversity and their roles are still underinvestigated. Here we present an ad hoc stratified sampling design and in-depth Illumina paired-end metabarcoding approach to explore microalgal diversity in lichen thalli of the model species *Ramalina farinacea* from different ecologies. Lichen thalli were surveyed according to three different sizes, and different thallus parts were considered for molecular, bioinformatics, and community diversity analyses. The results revealed that microalgal diversity strongly depends on the growth stage of the thalli, the geographic area, and the habitat type. The results also show that microalgal diversity does not vary along the thallus branches (lacinias)—that is, it does not correlate with the apical growth and founder effects—and that there is no balanced co-presence of two main photobionts as previously established in *R. farinacea*. The sampling design performed here minimizes bias in the assessment of photobiont diversity in lichens and is proposed to be reliable and applicable to further study microalgal diversity in lichen symbioses.

Key index words: **high-throughput sequencing; metabarcoding; mycobiont; photobiont; symbiosis; *Trebouxia***

***Abbreviations*: A, apical; ASVs, amplicon sequence variants; B, basal; BI, Bayesian inferences; eDNA, environmental DNA; HTS, High-throughput sequencing; IP, Iberian Peninsula; LP, La Palma; M, middle; ML, Maximum Likelihood; nrITS DNA, nuclear internal transcribed spacer region; OTUs, operational taxonomic units; PCoA, Principal Coordinates Analysis; PPs, posterior probabilities; SAG, Culture Collection of Algae at Göttingen University; TNF, Tenerife; UTEX, Culture Collection of Algae at the University of Texas**

Lichen symbioses are microecosystems in which multispecies assemblages are hosted in a three-dimensional structure, the lichen thallus, formed by the two major lichen symbionts, that is, the mycobiont (fungal partner) and the photobiont (a population of photosynthetic green or blue-green algae, more specifically distinguished as phycobionts and cyanobionts, respectively). Many other fungi, non-photosynthetic bacteria and photosynthetic green microalgae co-inhabit within the lichen thalli, can give rise to the peculiar phenotypes and may contribute to the diverse patterns of secondary metabolites (Spribille 2018, Hawksworth and Grube 2020, Spribille et al. 2020). Though the roles of these additional symbionts to the whole lichen outcome are still largely unknown (Spribille 2018), they might contribute to the worldwide distribution of lichens in diverse, sometimes extreme, environments and favor them even to be dominant organisms in some ecosystems (Romeike et al. 2002). The capacity to adapt to many environmental conditions and to diversify into the so far 18,000 described species (Kirk et al. 2001, Lücking et al. 2016) has been correlated to the specific combinations formed by the mycobionts and the photobionts. Indeed, in some lichen species the co-evolution of both partners under certain ecologies seems to lead to their concerted diversification (Rambold et al. 1998, del Campo et al. 2013).

[1]Received 4 December 2020. Revised 11 January 2021. Accepted 13 January 2021.
[2]Author for correspondence: e-mail arantxa.molins@uv.es.
*These authors contributed equally to this work.
Editorial Responsibility: X. Johnson (Associate Editor)

A wide range of more or less specific associations between mycobionts and phycobionts has been described, and this often depends on the selectivity that the two partners show toward each other (as reviewed by Muggia et al. 2018). In general, the concept of partner selectivity refers to the selectivity of the mycobiont toward the phycobionts (Yahr et al. 2004, 2006); however, selectivity and specificity are currently regarded as multidirectional terms (Peksa and Škaloud 2011, and revised by Muggia et al. 2018). Many mycobionts associate with a wide range of green microalgal species of a certain genus (e.g., are "generalist"), whereas others are always found in association with the same phycobiont species, being "specialist" (Helms et al. 2001, Casano et al. 2011, Leavitt et al. 2013, 2015, 2016, Nyati et al. 2013, Muggia et al. 2014, Singh et al. 2017). Other studies have also shown that symbiont association depends on the type of growth substrates (Bačkor et al. 2010, Leavitt et al. 2013, Muggia et al. 2014), the reproduction mode of the fungus (Steinová et al. 2019), or climatic conditions that may be altered by global changes (Fernández-Mendoza et al. 2011, Marini et al. 2011, Peksa and Škaloud 2011, Leavitt et al. 2016, Singh et al. 2017, Dal Grande et al. 2018, Steinová et al. 2019).

The worldwide distribution of lichens was also hypothesized to be strongly correlated with the ecological specialization and the physiological performances of the phycobionts (Casano et al. 2011, Peksa and Škaloud 2011). This has been studied in some cosmopolitan lichens which show a low phycobiont specificity that allows them to establish successful symbioses with locally adapted phycobionts in a wide range of habitats (Muggia et al. 2014). At a local scale, it may be easier to detect patterns of specificity mainly influenced by the interaction between lichenized fungi and the photobionts available in the pool of algae colonizing the surrounding environment (Belinchón et al. 2015).

In lichens, phycobiont diversity has been so far mainly investigated by Sanger sequencing and focused on the best known, most widespread and most species-rich family of terrestrial, lichenized green microalgae, the Trebouxiophyceae, and in particular on the genus *Trebouxia* for which to date 29 species have been currently accepted (as revised by Muggia et al. 2018). However, studies frequently report new, previously unrecognized, species-level lineages, of which the vast majority still lack formal description (Leavitt et al. 2015, Muggia et al. 2020). Even recently, Xu et al. (2020) described a new clade provisionally named as the "clade D" representing a previously unrecognized lineage of *Trebouxia* symbiotic with the lichen *Cetrariella delisei*. Due to the complex environmental matrices that lichen thalli represent, the amount of material necessary for DNA extraction, and potential PCR amplification and sequencing biases caused by the presence of multiple co-inhabiting phycobionts, DNA barcoding using Sanger sequencing may lead to an underestimation of the whole phycobiont diversity. Indeed, the traditional Sanger sequencing may fail in detecting the less represented phycobionts, while this drawback is overcome by the implementation of high-throughput sequencing (HTS). Nowadays, an improved assessment of organismal diversity in lichens has been possible by applying eDNA (environmental DNA) metabarcoding analyses based on high-throughput sequencing of entire holobiome communities within a thallus (e.g., Bates et al. 2012, U'Ren et al. 2014, Fernández-Mendoza et al. 2017, Banchi et al. 2018). Only recently lichen-associated phycobiont communities were explored by eDNA metabarcoding approaches within the Mediterranean basin (Moya et al. 2017, Dal Grande et al. 2018).

In the past few years, the lichen *Ramalina farinacea* has proved to be a suitable reference and model species for studying green microalgal diversity in lichens, as it recurrently shows the co-occurrence of at least two phycobionts (*Trebouxia* sp. TR9 and *Trebouxia jamesii*) inside the thalli. *R. farinacea* is a shrubby, fruticose lichens, with long, broad to narrow, more or less flattened branches, usually rather stiff, which grows epiphytic on all kind of trees and shrubs worldwide in region with a mild humid climate (Brodo et al. 2001). The species reproduces asexually via diaspores called soredia (i.e., agglomerates of fungal hyphae and algal cells; Brodo et al. 2001). Some years ago, the occurrence of two major *Trebouxia* phycobionts was revealed co-living within *R. farinacea* using microscopy techniques, culture isolations, and molecular characterization with different genetic markers (del Campo et al. 2010, 2013), while Casano et al. (2011) have further demonstrated that these two phycobionts respond differently to abiotic stresses. This let speculate that their coexistence would be advantageous for the whole lichen (Casano et al. 2011) and was shown to represent a common phenomenon in cosmopolitan, ecologically adapted lichens (del Hoyo et al. 2011, Muggia et al. 2014). Later, Moya et al. (2017) detected a certain microalgal diversity along the thallus branches (lacinias) of *R. farinacea* and suggested that it may correlate with microenvironmental conditions at the thallus level.

Here we reconsidered the reference system *Ramalina farinacea* and explored if and to which extent, the diversity of microalgal communities correlates with (i) environmental conditions and geographic origin, (ii) stage of development of the thalli, and (iii) different thallus parts. To reach these aims, we sampled the lichen species in two ecologically different environments (i.e., the Canary Islands and the Iberian Peninsula) characterized by a humid Macaronesian and dry Mediterranean climate, respectively, and performed an *ad hoc* stratified sampling design and in-depth Illumina paired-end metabarcoding assay.

MATERIALS AND METHODS

Sampling and experimental design. The lichen *Ramalina farinacea* is characterized by a shrubby thallus made of several branches of homogenous length (as schematically represented in Fig. 1). The specimens were collected during September 2017 in the Canary Islands and the Iberian Peninsula, in particular in La Palma and Tenerife, and in Castellón (Comunidad Valenciana), respectively (Fig. 1A). Two localities in La Palma—Montaña Quemada (MQ; 28°37′21.75″ N, 17°50′32.95″ E) and San Isidro (SI; 28°37′35.04″ N, 17°48′33.19″ E)—two in Tenerife—Pista Ovejeros (O; 28°25′27.19″ N, 16°23′10.55″ E) and San José de los Llanos (LL; 28°19′49.14″ N, 16°46′19.83″ E)—and one in Castellón—Azuébar (A; 39°51′59.39″ N, 0°23′27.10″ E)—were selected, as they are abundant and visually undamaged from air pollution of *R. farinacea* occur.

In each locality, we selected five trees, which were numbered 1–5 (Fig. 1). On tree no. 1, we sampled two branches, numbered 1 and 2, respectively, while on trees no. 2–5 we sampled a single branch (Fig. 1B). On each branch, three thalli of *Ramalina farinacea* were collected for a total of 18 specimens in each locality. All branches were selected inside the tree canopy. As a population of *R. farinacea* is usually composed by thalli of different sizes, which correspond to the age of the thallus itself, and these younger and elder individuals are growing intermixed, we collected thalli of three sizes defined as follow: large (L: at least 5 cm long), medium (M: from 1 to 2 cm) and small (S: up to 1 cm long). In doing this, we aimed at considering the different developmental stages of the lichen for each sampled population. For each tree branch, we collected one large, one medium and one small thallus. Following the method of Moya et al. (2017) to potentially corroborate their hypothesis, each thallus was further divided into three parts: apical (A, corresponding to the branch tips), middle (M, central part of the branches) and basal (B, most basal part of the branches, next to the holdfast). In the case of trees no. 1 branch no. 1, the three parts of each thallus were both individually treated and pooled together—the pool was labeled as A + M + B (Fig. 1C). On the contrary, the three thallus parts (A, M, B) of the thalli from trees no. 1 branch 2 and from the other four trees no. 2–5 were only treated pooled together (A + M + B; Fig. 1D, Table S1 in the Supporting Information).

DNA extraction, mycobiont barcoding PCR and Sanger sequencing. The 90 collected thalli were cleaned with a sterile razor blade under a stereomicroscope to remove surface contaminations and were superficially sterilized following Arnold et al. (2009). Total genomic DNA was isolated and purified using the DNeasy Plant Mini kit (Qiagen, Hilden, Germany) following the manufacturer's instructions.

The fungal nuclear internal transcribed spacer region (nrITS DNA) was analyzed to confirm the identity of the mycobiont in all the 90 lichen thalli using the primer pair ITS1F (Gardes and Bruns 1993) and ITS4 (White et al. 1990). PCRs were performed as described in Moya et al. (2017).

Haplotype network analysis. The genetic diversity of the *Ramalina farinacea* mycobionts was studied with haplotype analysis of the nrITS marker on the basis of statistical parsimony analyses of all 90 sequences using the TCS program (Clement et al. 2002) implemented in PopART v.1.7 (Leigh and Bryant 2015).

Metabarcoding assay. Chlorophyta algal communities associated with the thalli were assayed using Illumina high-throughput sequencing of the first part of the ITS1 of the rRNA operon, proposed as a universal barcode across eukaryotic kingdoms (Coleman 2009). Amplicons for Illumina MiSeq sequencing were generated by nested PCR: in the first PCR the forward nr-SSU-1780 (Piercey-Normore and DePriest 2001) and the reverse ITS4 primers were used and 27 amplification cycles were run; in the second PCR three replicates were generated using algae specific primers nr-SSU-1780/5.8S (Moya et al. 2017) modified with Illumina overhang adaptors (forward overhang: 5′-TCGTCGGCAGCGTCAGATGTGTATAAGAGACAGCTGCGGAAGGATCATTGATTC; reverse overhang: 5′-GTCTCGTGGGCTCGGAGATGTGTATAAGAGACAGATCCGTTGTTGAGAGTTGTC) and 22 amplification cycles were run. Nested PCRs (25 μL) contained 2.5 μL of 10× buffer, 0.4 μM nr-SSU-1780/5.8S 2R primers, 0.2 mM dNTPs, and 0.6 U · μL^{-1} of ExTaq (Takara, Shiga, Japan), and sterile Milli-Q water was used to bring to volume. The PCR conditions were 1 cycle of 95°C for 2 min, (27/21) number of cycles of 94°C for 30 s, 56°C for 45 s, and 72°C for 1 min, and a final extension of 72°C for 5 min. These replicates were then pooled together. PCR reactions were performed as described in Moya et al. (2017) and were purified using AMPure XP beads (Beckman Coulter). Indexing PCR and the addition of Nextera sequence adapters were performed using Nextera XT Index kit (Illumina Inc., San Diego, CA, United States) following the protocol for Illumina L library preparation. Finally, a second purification step was carried out using AMPure XP beads and libraries were quantified and pooled together. The libraries were sequenced on an Illumina MiSeq platform using the MiSeq Reagent Kit v3 (paired end 2× 300 bp; Genomics Core Facility at the University of Valencia, Spain).

Bioinformatic analyses. Quality control analysis of the Illumina MiSeq paired-end reads was performed using FastQC v 0.11.8. Raw reads were processed using Quantitative Insights into Microbial Ecology 2 (QIIME2 v. 2018.11; Bolyen et al. 2019). Demultiplexed paired-end sequence reads were preprocessed using DADA2 (Callahan et al. 2016), a package integrated into QIIME 2 that accounts for quality filtering, denoising, joining paired ends, and removal of chimeric sequences. The first 20 bp were trimmed from forward and reverse reads before merging to remove adaptors. Unlike traditional methods of clustering sequences into operational taxonomic units (OTUs) according to a fixed threshold, DADA2 denoises data sets to resolve sequence variants that differ by as little as one nucleotide and are referred to as amplicon sequence variants (ASVs; Callahan et al. 2016, Callahan et al. 2017). Such ASV-based approach is now recommended since it provides reliable data sets with higher resolution (Callahan et al. 2017) and it was therefore performed here. We performed further data filtering by removing any ASV present with less than 1,000 reads in the entire data set. The final ASVs table contained a total of 156 ASVs (Table S2 in the Supporting Information). Online Blast (https://blast.ncbi.nlm.nih.gov/Blast.cgi) and phylogenetic analyses were used to infer the taxonomic assignment of each ASV. The resulting feature ASV table was used for α and ß-diversity analyses. Prior to statistical analysis of microalgae, we produced rarefaction curves in QIIME2 in order to choose an appropriate minimum rarefying depth (n = 3,000). We standardized the ASV table to generate measures of α-diversity and community composition for each sample by normalizing with the cumulative sum scaling (CSS, Paulson et al. 2013) implemented in QIIME 1.9 (Caporaso et al. 2010). For statistical analyses, core diversity metrics were analyzed for α-diversity including: Shannon's diversity index, phylogenetic diversity (Faith pd; Faith 1992), and the evenness index. The significance of α diversity was determined using Kruskal–Wallis test, which estimate the differences between groups, accepting only adjusted P-values < 0.05 as significant. Bray–Curtis dissimilarity distances and UniFrac distance metrics were calculated for the estimation of ß-diversity. The ß-diversity group significance

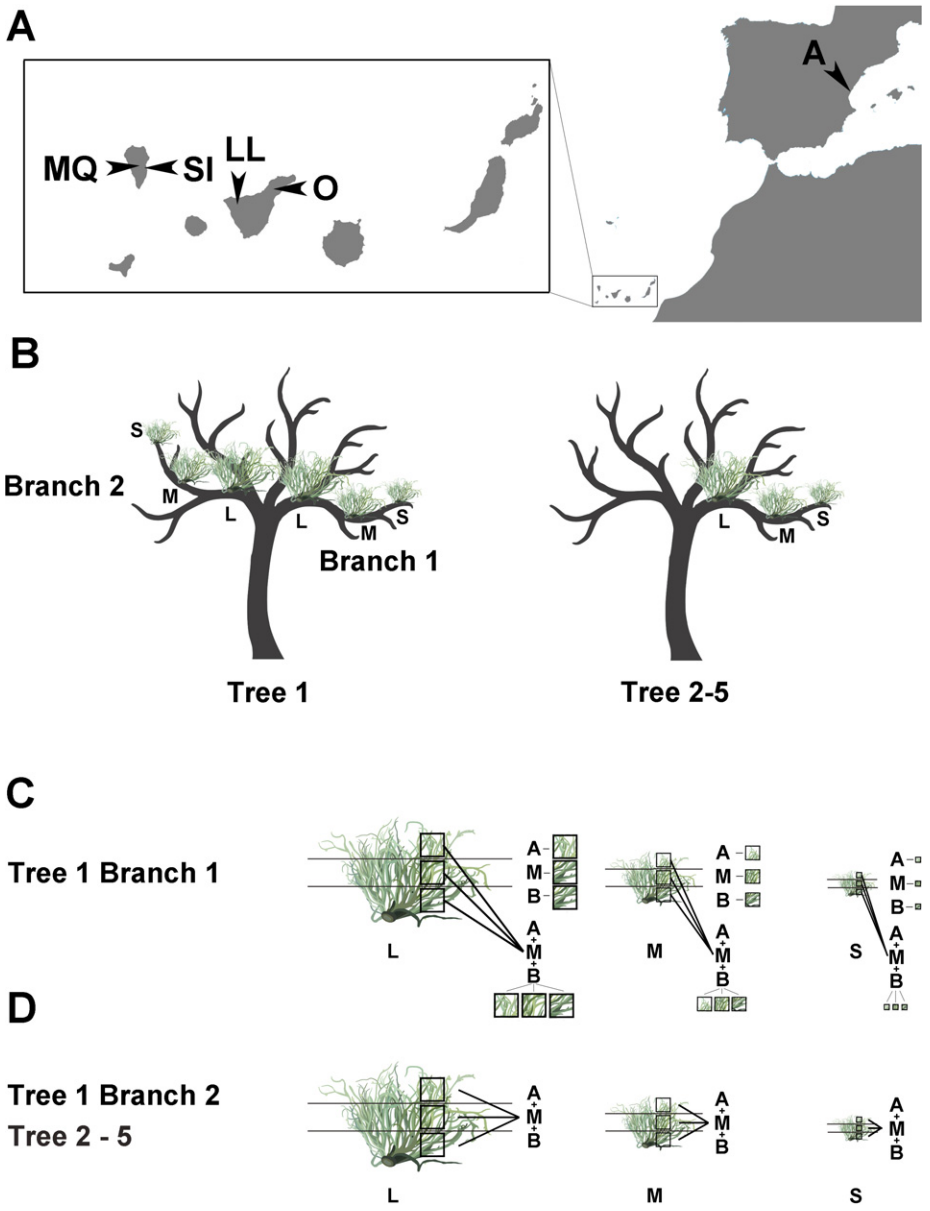

FIG. 1. (A) Geographic location of the sampling sites included in this study: Iberian Peninsula and the Canary Islands (MQ, Montaña Quemada; SI, San Isidro; LL, San José de los Llanos; O, Pista Ovejeros; A, Azuébar). (B) Preparation of lichen material prior to DNA extraction: In each locality, we selected five trees, which were numbered 1–5. On tree no. 1, we sampled two branches, numbered 1 (C) and 2 (D), respectively, while on trees no. 2–5 (D) we sampled a single branch. The three thalli of *Ramalina farinacea* were selected according to three different sizes: large (L), medium (M), and small (S). Each thallus was further divided into three parts: apical (A), middle (M), and basal (B). (C) In the case of tree no. 1 branch no. 1, the three parts of each thallus were both individually treated (A, M, B) and pooled together (A + M + B). (D) The three thallus parts (A, M, B) of the thalli from tree no. 1 branch 2 and from the other four trees no. 2–5 of each site were only treated pooled together (A + M + B). [Colour figure can be viewed at wileyonlinelibrary.com]

test was done using a permutational ANOVA (PERMANOVA) pairwise test for the distance matrix via 9,999 Monte Carlo permutations, and false discovery rate multiple correction.

Phylogenetic assignment of Trebouxia *ASVs.* The identity of *Trebouxia* ASVs was further check by phylogenetic assignment. The sequence alignment was prepared including: (i) the *Trebouxia* ASVs sequences, (ii) selected sequences published by Leavitt et al. (2015) and Moya et al. (2017), (iii) the first match of blast search against whole GenBank database for each ASV, (iv) a selection of *Trebouxia* type species available from the Culture Collection of Algae at Göttingen University (SAG), from the Culture Collection of Algae at the University of Texas (UTEX) and reference sequences of *Trebouxia* sp. TR9 (FJ418565). The alignment was automatically performed using MAFFT v 7.0 (Katoh et al. 2002, Katoh and Toh 2008) using default parameters. The best-fit substitution model for the ITS1 region (TVM + G) was chosen using jModelTest v 2.0 (Darriba et al. 2012), by applying the Akaike information criterion (Akaike 1974). Maximum likelihood (ML) analysis was implemented in RAxML v 8.1.11 (Stamatakis 2006) using the GTRGAMMA substitution model. Bootstrap support was calculated based on 1,000 replicates (Stamatakis et al. 2008).

Bayesian inferences (BI) were carried out in MrBAYES v 3.2 (Ronquist et al. 2012) using two parallel runs with six chains over 20 million generations, starting with a random tree and sampling every 200 steps. We discarded the first 25% of data as burn-in and the corresponding posterior probabilities (PPs) were calculated from the remaining trees. MAFFT, jModelTest, ML, and BI analyses were implemented at the CIPRES Science Gateway v 3.3 webportal (Miller et al. 2010).

The new sequences are available with the NCBI accession numbers MN684367-MN684494 (file SUB6536154).

RESULTS

Sanger sequencing and diversity of mycobiont genotypes. The identity of the mycobiont *Ramalina farinacea* was confirmed for all the samples by BLAST searches against the GenBank database. Out of the 90 collected individuals, a total of 24 ITS haplotypes were recognized, two of which, that is, haplotype no. 1 and no. 2, are the most common, being shared among 59 and 22 thalli, respectively (Fig. S1 in the Supporting Information). Haplotype 1 only included Canarian thalli while haplotype 2 included thalli from both Iberian Peninsula and Canary Islands; 14 thalli from the Canary Islands and only one from the Iberian Peninsula are characterized by their own haplotype. Also, the single locality in the Iberia Peninsula (Azuébar) present only two haplotypes, while the haplotype diversity in the Canary Islands is much higher, as up to 11 haplotyes are identified in one population (San José de los Llanos; Fig. S1).

Microalgal metabarcoding. A total of 8,869,009 internal transcribed spacer 1 (ITS1) raw reads were generated, of which 8,729,896 passed the demultiplexing step and quality filter. This represented a mean of 64,665 (median 60,409) algal reads per sample, with a minimum of 3,233 (in sample O25) and a maximum of 143,454 (in sample LL13) reads per sample (Table S1). After filtering the ASVs represented by less than 1,000 reads, the data set was comprised of 156 ASVs (Table S2). These ASVs were classified by blast into *Trebouxia* spp. (98.6% reads), *Asterochloris* spp. (0.02%), and seven other green microalgale taxa (1.4%; Tables S2 and S3 in the Supporting Information).

Taxonomic assignment of the microalgal taxa. In the 135 samples, we detected a total of ten *Trebouxia* species or taxonomic units by performing both blast identity search and phylogenetic analyses (Fig. S2 in the Supporting Information, Tables S2 and S3). The aligned *Trebouxia* ITS1-5.8S fragment was 268 bp in length. BI and ML phylogenetic hypotheses were topologically congruent and also consistent with previous studies (Muggia et al. 2010, 2014, 2018, Leavitt et al. 2015, Voytsekhovich and Beck 2016). According to the clade nomenclature introduced for *Trebouxia* by Leavitt et al. (2015), and subsequently applied by Moya et al. (2017) and Muggia et al. (2020), ASVs of eight *Trebouxia* species belong to clade A, precisely: *T. asymmetrica*, *T. cretacea*, *T. decolorans*, *T. jamesii*, *T. vagua*, *Trebouxia* sp. TR9, *Trebouxia* sp. A54 (MN622995), and *Trebouxia* sp. A57 (MH035958). The remaining two *Trebouxia* were placed in clade S (*T. simplex*; i.e., ASV1), and in clade C (*T. corticola*; i.e., ASV119 and ASV31). *Trebouxia cretacea*, *T. simplex,* and *Trebouxia* sp. A54, were represented by a unique ASV (Fig. S2 in the Supporting Information). *Trebouxia* sp. TR9 and *T. jamesii*, which showed the highest number of reads (4,862,672 and 696,149, respectively), were represented by 14 and five ASVs, respectively (Table S2). *Trebouxia vagua* and *T. asymmetrica* (which had 314,760 and 452,497 total reads, respectively) were represented by 39 and 56 ASVs, respectively, *Asterochloris glomerata* was the only species detected for this genus and is represented by ASV149 (Table S3).

Sequences of other green microalgal genera included *Appatococcus*, *Coccomyxa, Diplosphaera, Elliptochloris*, *Stichococcus.*

Eleven ASVs (130, 131, 133, 135, 136, 137, 139, 142, 143, 145, and 151) did not produced any match with known taxa in the blast search in the NCBI database, and thus, no identity could be assigned.

Relative abundance of Trebouxia *by geographic region and sample.* The composition of *Trebouxia* species strongly varied between the Canary Islands and Iberian Peninsula (Fig. 2). *Trebouxia jamesii* was predominant in the thalli of the Iberian Peninsula (more than 50% of reads in each sample), whereas *Trebouxia* sp. TR9*, T. vagua,* and *T. asymmetrica* were here represented by only up to 10% of reads (Fig. 2, Table S3). On the contrary, *Trebouxia* sp. TR9 dominated in the thalli from the Canary Islands with more than 80% of reads in the four localities. Of the total ten *Trebouxia* species detected in the whole sampling (Fig. 2), *Trebouxia* sp. A54, *T. corticola,* and *T. simplex* were recovered only in the Canary Islands.

In the Iberian Peninsula, the composition of *Trebouxia* taxa showed a uniform pattern in 14 samples, in which more than 60% of reads corresponded to *T. jamesii* (Fig. S3A in the Supporting Information). *Trebouxia* sp. TR9 was dominant only in three samples (A17, A18 and A19; Fig. S3A, Table S1), while in the remaining ten samples *T. asymmetrica* and *T. vagua* dominated.

In Tenerife, *Trebouxia* sp. TR9 dominated (more than 60% reads) in 45 samples out of the total 54 (Fig. S3B). Only in samples O12 and O21, *T. asymmetrica* and *T. jamesii* were recovered as the most abundant phycobionts, respectively. In the remaining seven samples, both *T. asymmetrica* and *T. vagua* were abundant in five samples, while *T. decolorans* was mostly abundant in samples O6 and O9. Only in samples LL2, LL16, LL24, LL25, and LL26, *T. asymmetrica* was recovered as the most abundant phycobiont.

In La Palma, 43 samples of the total 54 shared the same pattern recovered for the Tenerife samples

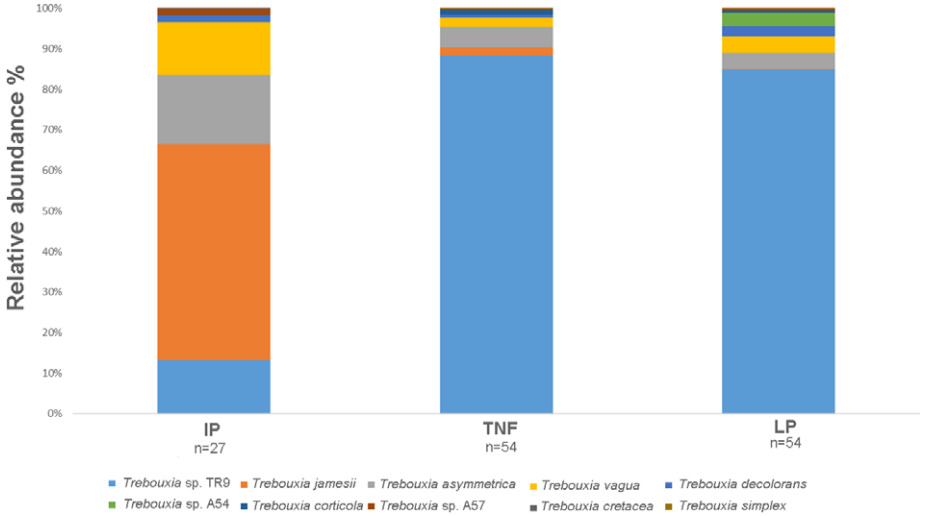

FIG. 2. Graphs of mean relative abundance of *Trebouxia* species stratified by region (IP, Iberian Peninsula; TNF, Tenerife; and LP, La Palma).

(Fig. S3C). Only in samples MQ21, SI5, and SI11, the dominant microalgae were *Trebouxia* sp. A54 and *T. decolorans*. Seven samples presented *T. asymmetrica, T. vagua,* and *T. decolorans* in major amount while SI4 completely lacked *T. decolorans*.

Relative abundance of Asterochloris *and other green microalgae by region. Asterochloris glomerata* was five times more represented in the Iberian Peninsula than in the Canary Islands (Table S3).

In the group "other green algae," a total of seven microalgae were included. All those taxa were detected in Canary Islands, whereas only four in Iberian Peninsula (Table S3). In more detail, *Coccomyxa viridis*, *Elliptochloris subphaerica,* and *Stichococcus* sp. were found in the Canary Islands and in Iberian Peninsula, *Appatococcus* sp., *Coccomyxa antarctica,* and *Coccomyxa* sp. were exclusively found in Canary Islands, while *Diplosphaera* sp. was found to occur only in the Iberian Peninsula (Table S3).

α-diversity of total microalgal community. Shannon's diversity index (Fig. 3, A and B), the evenness index (Fig. 3, C and D), and phylogenetic diversity (Faith pd; Fig. 3, E and F) calculated for the microalgal community according to thallus size indicated that the α-diversities for small thalli (0–1 cm) was significantly higher (in Shannon and evenness Index) than those found in thalli of large and medium sizes (Table S4 in the Supporting Information). The diversity of the algal communities was higher in the basal zone of the thallus branches than in the apical or middle zones treated individually (though not statistically supported; Table S4), while apical and middle zones showed individually similar diversity values to the pooled AMB sample (Fig. 3).

ß-diversity of total microalgal community. The principal coordinates analysis (PCoA) plots for samples from all the five localities treated as pooled AMB and collected from the tree no. 1, branches 1 and 2, did not show any significant differences between branches. ß-diversity for samples treated as AMB, considering all the five trees analyzed in each locality, indicates that if only one tree was sampled, we would not recover the whole algal diversity of the area (Fig. S4, Table S5 in the Supporting Information).

PCoA plots showed that samples were strongly clustered based on the geographic region (statistically significant; Table S6 in the Supporting Information), for example, samples from Iberian Peninsula (continental) clearly segregated from those of Tenerife and La Palma (insular; Fig. 4), independent to the tree or branch analyzed.

DISCUSSION

Metabarcoding of lichen photobionts. In the past few years, high-throughput sequencing (HTS) technologies combined with eDNA metabarcoding analyses have increasingly expanded to describe and compare the diversity of microbial communities in a multiplicity of environments and under diverse ecological conditions. The HTS techniques have surpassed and almost substituted the traditional Sanger sequencing because of their greater depth and resolution in the taxonomic assessment of multiple taxa at once, beside its lower costs. In this context, lichen symbioses have represented suitable microniches for the application and testing the performance of HTS and metabarcoding to uncover the previously unknown species diversity of bacteria, fungi, and algae inside the thalli (Grube et al. 2015, Cernava et al. 2017, Fernández-Mendoza et al. 2017, Moya et al. 2017, Banchi et al. 2018, Paul et al. 2018). Thus, the identification of multiple organisms co-inhabiting a lichen thallus (Grube et al.

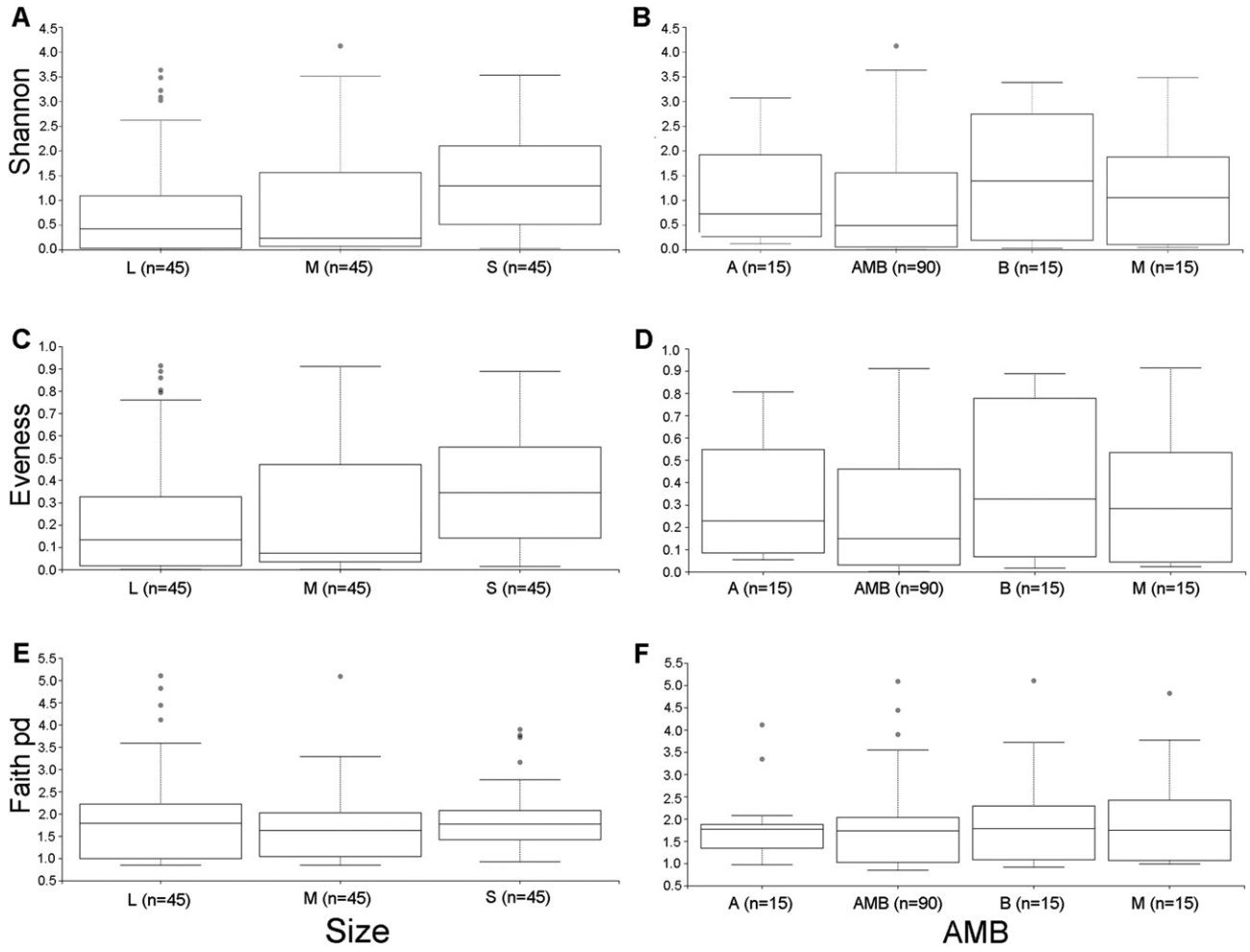

FIG. 3. Microalgal diversity in thalli of *Ramalina farinacea*: (A, B) α-diversity boxplots representing Shannon's diversity index, (C, D) evenness index, and (E, F) phylogenetic diversity (Faith pd) between all *R. farinacea* samples analyzed by thallus size (A, C and E) and by thallus parts (AMB; B, D, and F). Sizes of thalli: large (L: at least 5 cm long), medium (M: from 1 to 2 cm), and small (S: up to 1 cm long). Parts of thalli: apical (A, corresponding to the branch tips), middle (M, central part of the branches), and basal (B, most basal part of the branches, next to the holdfast). In the case of three parts of each thallus were pooled together, labeled as AMB.

2009, Casano et al. 2011, Muggia and Grube 2018, U'Ren et al. 2019, Smith et al. 2020) has overcome the traditional paradigm of "one fungus associated with one alga", which has described the lichen symbioses for over a century. Nevertheless, the functions of these associated bacteria, fungi, and algae co-inhabiting lichen thalli have not been investigated yet, and the two major players of a lichen symbiosis are still recognized to be the mycobiont and the photobionts (i.e., the principal, biologically relevant, green or blue-green algae; Honneger 1992).

Recently, Paul et al. (2018) compared the utility of Sanger sequencing and HTS metabarcoding for inferring photobiont diversity in lichens. The multiplicity of phycobionts in lichen thalli, indeed, has been specifically addressed by HTS and metabarcoding so far only by the two studies of Moya et al. (2017) and Dal Grande et al. (2018) in two different lichen symbioses. However, it was detected previously by culture approaches (Casano et al. 2011, Muggia et al. 2014) or by the use of different primers and conditions in PCR amplifications with subsequent Sanger sequencing (Singh et al. 2017, Molins et al. 2018). Though Sanger sequencing still remains the most appropriate technique to identify the principal phycobiont (i.e., the biologically relevant algae characterizing a certain lichen symbiosis, see above), HTS is certainly the most suitable approach to obtain the taxonomically most comprehensive data sets of lichen symbionts to describe their diversity and to model patterns of interactions under diverse ecologies (Paul et al. 2018, U'Ren et al. 2019).

The importance of species identification in metabarcoded samples. Though the molecular identification of the lichen mycobiont species may be bypassed in metabarcoding studies aiming at describing algal, bacterial, and/or fungal-associated communities, this step should not to be undervalued and its importance has been stressed recently (Dal Grande

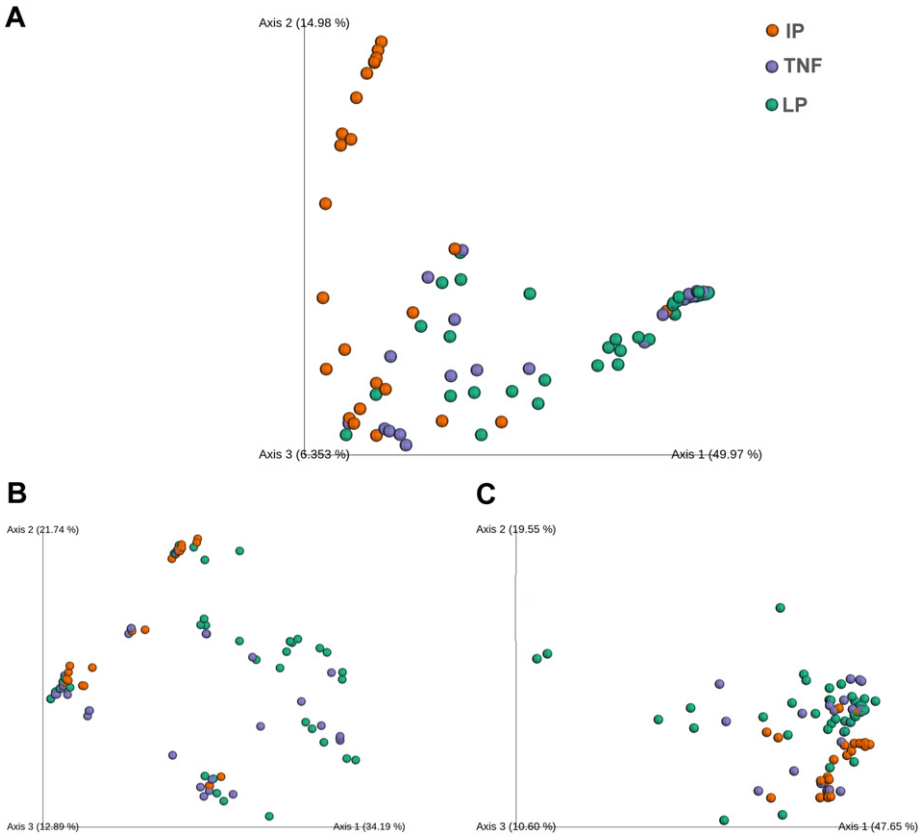

FIG. 4. Principal coordinates analysis (PCoA) based on Bray–Curtis (A), unweighted UniFrac distance (B), and weighted UniFrac distance (C) of microalgal communities for all samples (n = 135) (samples colored by region IP, Iberian Peninsula; TNF, Tenerife; and LP, La Palma).

et al. 2017, 2018, Onuț-Brännström et al. 2018). Indeed, the subtle genotypic differences that can be detected in the mycobionts can lead to or be correlated with the variation detected in the associated photobionts. Hence, the identity and the genetic variation of the mycobiont *Ramalina farinacea* was here assessed by Sanger sequencing and studied by haplotype network analysis. Mycobiont genotype diversity was found to correlate with the geographic origin of thalli (Fig. S1). These results are in accordance with del Campo et al. (2013), and a more detailed analysis including additional localities should likely confirm this pattern.

It is a common practice to perform the taxonomic assignment of the sequenced reads based on the hits obtained from a blast search against a comprehensive sequence database. A more reliable taxonomic assignment can be performed by phylogenetic analyses in which the diversity of the ASVs is compared in an evolutionary framework with that of other related taxa. Though this approach may be criticized because the sequence length of the ASVs (about 300 bp) is much shorter than that of the genetic markers traditionally used for phylogenetic reconstructions (ranging at about 600 bp), it proves useful to confirm the identification of the taxa. Further, the comparison within an evolutionary frame is even more important for the identification of *Trebouxia* species/taxonomic units, as no sequence reference database (i.e., Greengenes, DeSantis et al. 2006; UNITE, Nilsson et al. 2018; SILVA, Quast et al. 2013) is available for this group of algae, but reference lineages have been proposed for their phylogenetic assignment (Leavitt et al. 2015, Muggia et al. 2020). Thus, the phylogenetic species identification of the *Trebouxia* ASVs was performed in the present study, and this highlighted the presence of two still unnamed (undescribed) lineages, within the *Trebouxia* clade "A," namely *Trebouxia* sp. A54 and *Trebouxia* sp. A57, whereas all the other ASVs could be confirmed to belong to already known *Trebouxia* species.

Trebouxia *and microalgal diversity correlates with geographic origin of the thalli.* *Trebouxia* species diversity and its composition inside the thalli of *Ramalina farinacea* was observed to correlate with the geographic origins of the samples. In thalli from Iberian Peninsula, *Trebouxia jamesii* was the principal photobiont, while *Trebouxia* sp. TR9, *T. vagua,* and *T. asymmetrica* were detected in minor amount. Alternatively, in the Canary Islands the mycobiont showed a stronger association with *Trebouxia* sp.

TR9. In general, thalli of the Canary Islands also presented a higher diversity of *Trebouxia* species than those from Iberian Peninsula, as three more *Trebouxia* species or taxonomic units have been found, that is, *Trebouxia* sp. A54, *T. corticola,* and *T. simplex*. The preference of continentality and insularity of the two principal photobionts *T. jamesii* (TR1) and *Trebouxia* sp. TR9, respectively, was already highlighted by del Campo et al. (2013). However, due to the Sanger sequencing approach adopted by the authors (del Campo et al. 2013), the differences in the community composition of the other associated *Trebouxia* species could not be highlighted at that time, instead it is here, thanks to the application of the metabarcoding approach.

Previous studies performed on *Ramalina farinacea* holobionts from different localities always reported the balanced presence of two predominant, biologically relevant photobionts, that is, *Trebouxia jamesii* and *Trebouxia* sp. TR9 (del Campo et al. 2010, 2013, Casano et al. 2011, Moya et al. 2017). This let considered the lichen *R. farinacea* a particular case in which a fungal species specifically associates with two different *intrathalline Trebouxia* phycobionts (*Trebouxia* sp. TR9 and *Trebouxia jamesii*) however, the stratified sampling and deep sequencing performed in this study offer a new, different, perspective on the association patterns of the mycobiont and its two phycobionts. Considering that the results of the Sanger sequencing have usually identified the most biologically relevant phycobiont in lichen thalli (Paul et al. 2018), the HTS metabarcoding in the present case of *R. farinacea* further supports this outcome. As a consequence of this, the sequencing results rebut the balanced, co-presence of the two main photobionts stated previously, because either one or the other *Trebouxia* species is predominantly present in individual thalli. In 33% of the samples, the balanced co-presence of the two predominant microalgae was confirmed but in the remaining 67% it was not; the lack of a balanced co-presence was mainly observed also in the samples from the Canary Islands.

Interestingly, among all the samples, the genetic, intraspecific diversity of each principal photobiont *Trebouxia jamesii* and *Trebouxia* sp. TR9 is rather low, being the number of their corresponding ASVs much lower than that recovered for the other associated *Trebouxia* species (i.e., *T. vagua* and *T. asymmetrica*). It might be speculated that co-evolution of the *Ramalina* mycobiont with its two specific photobionts has been responsible of the homogenization of their genotypes. On the contrary, the high number of ASVs recovered for *T. vagua* and *T. asymmetrica* might represent erroneous sequences having one or a few mismatches with the original sequence and causing therefore false-positive genotypes, an event that has been already observed in few other studies (Mark et al. 2016, Gueidan et al. 2019). Also, the diversity among the ASVs of *T. vagua* and *T. asymmetrica* might be attributed to the multiple copies in which the ITS occurs in the genome, highlighting in this way the number of potential paraloga in these two species. Previous results obtained with 454 sequencing detected a similar intraspecific diversity for *T. asymmetrica* but not for *T. vagua* (Moya et al. 2017).

The community composition of the other microalgae associated with the *Ramalina farinacea* also mirrors a geographic pattern. *Asterochloris glomerata* is five times more represented in the Iberian Peninsula than in the localities of the Canary Islands (Table S3), while *Diplosphaera* sp. was exclusively found in the Iberian Peninsula. Alternatively, *Coccomyxa antarctica* and *Coccomyxa* sp. were found only in La Palma. The two localities in La Palma also showed the highest number of microalgal taxa (6).

In each locality, the sampling performed on five trees did not reveal any microalgal diversity either among the trees or among thalli on the different branches of the same tree (for trees no. 1). However, the sampling procedure demonstrates the importance of sampling multiple thalli of different growth sizes on multiple trees to catch the most comprehensive diversity of microalgal community associated with a lichen species in a certain area.

Diversity of Trebouxia *and other microalgae correlates with the growth of the thalli.* In a previous metabarcoding study, Moya et al. (2017) speculated that the diversity of microalgae in thalli of *Ramalina farinacea* correlates to the different parts of the thallus, being the apical zone of the thallus branches algae-richer than the basal parts. However, the present results do not confirm this hypothesis; no significant variation in microalgal diversity was recovered along the middle and apical parts, but in contrast we recovered a slightly higher microalgal diversity in the basal parts of the branches (not significant). On the contrary, the stratified sampling shows that there is a significant diversity in microalgal composition/communities between young and old thalli, being young thalli (i.e., the smallest in the sampling) those hosting the highest microalgal diversity. Also, the observed microalgal diversity is consistent with the geographic origin of the samples. This pattern suggests that there is a sort of selection toward the algae becoming the principal phycobiont of *R. farinacea* during the growth and the establishment of the thallus in a certain habitat. At the same time, there is a general, progressive decrease of total microalgal diversity in the thalli, though maintaining the differentiation of community composition between insular and continental samples.

The "phycobiont selection" process observed here has remained hidden until now because previous studies did not considered thalli in different growth stages, while only Moya et al. (2017) analyzed different thallus parts but using a single thallus of *Ramalina farinacea*. The applied sampling procedure and the present results clearly strengthen the perception

that estimation of microalgal diversity, and of the overall assessment of the main phycobiont, can be considerably biased. If the sampling would include only small thalli, this would lead to an overestimation of the microalgal diversity. Although the results were not statistically supported, the diversity of the algal communities was higher in the basal zone of the thallus branches than in the apical or middle zones treated individually. Therefore, taking only either the basal, the central or the apical part of the thallus branches for DNA extraction would lead to an incorrect estimation of the total microalgal diversity in a thallus in its different stages of development. Still, it is hardly possible to pre-define the optimal number of samples that should be analyzed to reliably assess microalgal diversity in a lichen species, as it often correlates with the aim of the study. Notwithstanding this, our results show that at least multiple thalli (here five were sampled) with different sizes (here three sizes were considered) of a certain species should be considered to better estimate the microalgal diversity potentially associated with that lichen holobionts.

The habitat shapes, the mycobiont selects. Lichens are nowadays known to be cradles of a still uncovered diversity of microorganisms (Arnold et al. 2009, Grube et al. 2009, Muggia and Grube 2018). In particular, microalgal communities associated with the thalli of the lichen *Ramalina farinacea* varies among different environments and according to the developmental stage of the thallus. The patterns detected in *R. farinacea* suggest that selection of the main phycobiont is taking place in the thalli during its growth. Among the pool of microalgae that the mycobiont encounters on the substrate and that it incorporates into the thallus during the first years of growth, there is one microalgae, which is enhanced to become the biological relevant photobiont in the symbiosis, while the others are progressively reduced and will likely play no significant role. This phenomenon recalls the famous citation of "Everything is everywhere, but the environment selects" by Baas Becking (1934), who has coined it to describe the mechanisms of natural community assemblies. In the original definition, indeed, the author (Baas Becking 1934) meant that all microbial life is distributed worldwide, but in a given environmental setting most of the microbial species are only latently present and can remain hidden to our perception because they occur at densities below our limit of detection (De Wit and Bouvier 2006). This concept fits here for *R. farinacea*, as the presence of the less abundant microalgae has been masked by the detection of the principal, predominant phycobiont. The diversity of these additional microalgae and their community composition in different environments (i.e., continental Mediterranean *vs.* insular Macaronesian) is uncovered only when an in-depth, stratified sampling is performed at the microscale of individual lichen thalli. In the case of *R. farinacea*, it seems that the environment shapes the microalgal communities (phycobiont pool) but the lichen mycobiont is the one which selects the most suitable microalgae to become the specialized partner of its symbiotic relationship. This seems even to correlate with, or be potentially driven by the genotype of the mycobionts. In lichens, different degree of mycobiont-photobiont specificity is known (Leavitt et al. 2015, Beck et al. 2019, Steinová et al. 2019), and in some cases, these relationships have been correlated to the suitability and the physiological performance of the photobionts in diverse, or even changeable, environmental settings (Vančurová et al. 2018, Steinová et al. 2019). The mycobiont *R. farinacea* seems to behave first as a generalist species, which associate with several phycobionts at the beginning of its symbiotic life, and secondly become more specialist restricting his choice to the phycobionts, which likely has the best fitness for the environment in which that holobiont develops.

ACKNOWLEDGEMENTS

Funding for field and laboratory work for this study was provided by the Ministerio de Economia y Competitividad (MINECO and FEDER, Spain) (CGL2016-79158-P), Prometeo Excellence in Research Program (Generalitat Valenciana, Spain) (PROMETEOII/2013/021, PROMETEO/2017/039). Dr. Giuseppe D'Auria from FISABIO-SP (Valencia) helped with bioinformatics analysis. Dr. Arnoldo Santos (Tenerife) was involved in the design of the surveys and the collection of samples in Tenerife and La Palma Islands, and Dr. Salvador Chiva for the haplotype network. We would like to thank Drs. Pavel Škaloud (Charles University, Prague) and Pradeep Divakar (Universidad Complutense de Madrid) for their expert comments.

REFERENCES

Akaike, H. 1974. A new look at the statistical model identification. *IEEE T. Autom. Cont.* 19:716–23.

Arnold, A. E., Miadlikowska, J., Higgins, K. L., Sarvate, S. D., Gugger, P., Way, A., Hofstetter, V., Kauff, F. & Lutzoni, F. 2009. A phylogenetic estimation of trophic transition networks for ascomycetous fungi: are lichens cradles of symbiotrophic fungal diversification. *Syst. Biol.* 58:283–97.

Baas Becking, L. G. M. 1934. *Geobiologie of inleiding tot demilieukunde.* W.P. Van Stoc-kum and Zoon, The Hague, the Netherlands (in Dutch), 136 pp.

Bačkor, M., Peksa, O., Škaloud, P. & Backorová, M. 2010. Photobiont diversity in lichens from metal-rich substrata based on ITS rDNA sequences. *Ecotox. Environ. Safe* 73:603–12.

Banchi, E., Ametrano, C. G., Stanković, D., Verardo, P., Moretti, O., Gabrielli, F., Lazzarin, S. et al. 2018. DNA metabarcoding uncovers fungal diversity of mixed airborne samples in Italy. *PLoS ONE* 13:e0194489.

Bates, S. T., Berg-Lyons, D., Lauber, C. L., Walters, W. A., Knight, R. K. & Fierer, N. 2012. A preliminary survey of lichen associated eukaryotes using pyrosequencing. *Lichenologist* 44:137–46.

Beck, A., Bechteler, J., Casanova-Katny, A. & Dzhilyanova, I. 2019. The pioneer lichen *Placopsis* in maritime Antarctica: genetic diversity of their mycobionts and green algal symbionts, and their correlation with deglaciation time. *Symbiosis* 79:1–24.

Belinchón, R., Yahr, R. & Ellis, J. E. 2015. Interactions among species with contrasting dispersal modes explain distributions for epiphytic lichens. *Ecography* 38:762–8.

Bolyen, E., Rideout, J. R., Dillon, M. R., Bokulich, N. A., Abnet, C. C., Al-Ghalith, G. A., Alexander, H. et al. 2019. Reproducible, interactive, scalable and extensible microbiome data science using QIIME 2. *Nat. Biotechnol.* 37:852–7.

Brodo, I. M., Sharnoff, S. D. & Sharnoff,, S. 2001. *Lichens of North America*. Yale University Press, New Haven - London, 795 pp.

Callahan, B. J., McMurdie, P. J. & Holmes, S. P. 2017. Exact sequence variants should replace operational taxonomic units in marker-gene data analysis. *ISME J.* 11:2639–43.

Callahan, B. J., McMurdie, P. J., Rosen, M. J., Han, A. W., Johnson, A. J. & Holmes, S. P. 2016. DADA2: high resolution sample inference from amplicon data. *Nat. Methods* 13:581–3.

Caporaso, J. G., Kuczynski, J., Stombaugh, J., Bittinger, K., Bushman, F., Costello, E. K., Fierer, N. et al. 2010. QIIME allows analysis of high-throughput community sequencing data. *Nat. Methods* 7:335–6.

Casano, L. M., del Campo, E. M., García-Breijo, F. J., Reig-Armiñana, J., Gasulla, F., del Hoyo, A., Guera, A. & Barreno, E. 2011. Two *Trebouxia* algae with different physiological performances are ever-present in lichen thalli of *Ramalina farinacea*. Coexistence versus competition? *Environ. Microbiol.* 13:806–18.

Cernava, T., Erlacher, A., Aschenbrenner, I. A., Krug, L., Lassek, C., Riedel, K., Grube, M. & Berg, G. 2017. Deciphering functional diversification within the lichen microbiota by metaomics. *Microbiome* 5:82.

Clement, M., Snell, Q., Walke, P., Posada, D. & Crandall, K. 2002. TCS: estimating gene genealogies. *Proc. 16th Int. Parallel Distrib. Process Symp.* 2:184.

Coleman, A. W. 2009. Is there a molecular key to the level of biological species in eukaryotes? A DNA guide. *Mol. Phylogenet. Evol.* 50:197–203.

Dal Grande, F., Rolshausen, G., Divakar, P. K., Crespo, A., Otte, J., Schleuning, M. & Schmitt, I. 2018. Environment and host identity structure communities of greenalgal symbionts in lichens. *New Phytol.* 217:277–89.

Dal Grande, F., Sharma, R., Meiser, A., Rolshausen, G., Büdel, B., Mishra, B., Thines, M., Otte, J., Pfenninger, M. & Schmitt, I. 2017. Adaptive differentiation coincides with local bioclimatic conditions along an elevational cline in populations of a lichen-forming fungus. *BMC Evol. Biol.* 17:93.

Darriba, D., Taboada, G. L., Doallo, R. & Posada, D. 2012. jModelTest 2: more models, new heuristics and parallel computing. *Nat. Methods* 9:772.

De Wit, R. & Bouvier, T. 2006. 'Everything is everywhere, but, the environment selects', what did Baas Becking and Beijerinck really say? *Environ. Microbiol.* 8:755–8.

del Campo, E., Casano, L. M., Gasulla, F. & Barreno, E. 2010. Suitability of chloroplast LSU rDNA and its diverse group I introns for species recognition and phylogenetic analyses of lichen-forming *Trebouxia* algae. *Mol. Phylogenet. Evol.* 54:437–44.

del Campo, E. M., Catalá, S., Gimeno, J., del Hoyo, A., Martínez-Alberola, F., Casano, L. M., Martin, G. & Barreno, E. 2013. The genetic structure of the cosmopolitan three-partner lichen *Ramalina farinacea* evidences the concerted diversification of symbionts. *FEMS Microbiol. Ecol.* 83:310–23.

del Hoyo, A., Álvarez, R., del Campo, E. M., Gasulla, F., Barreno, E. & Casano, L. M. 2011. Oxidative stress induces distinct physiological responses in the two *Trebouxia* phycobionts of the lichen *Ramalina farinacea*. *Ann. Bot.* 107:109–18.

DeSantis, T. Z., Hugenholtz, P., Larsen, N., Rojas, M., Brodie, E. L., Keller, K., Huber, T., Dalevi, D., Hu, P. & Andersen, G. L. 2006. Greengenes, a chimera-checked 16S rRNA gene database and workbench compatible with ARB. *Appl. Environ. Microb.* 72:5069–72.

Faith, D. P. 1992. Systematics and conservation: on predicting the feature diversity of subsets of taxa. *Cladistics* 8:361–73.

Fernández-Mendoza, F., Domaschke, S., García, M. A., Jordan, P., Martín, M. P. & Printzen, C. 2011. Population structure of mycobionts and photobionts of the widespread lichen *Cetraria aculeata*. *Mol. Ecol.* 20:1208–32.

Fernández-Mendoza, F., Kopunt, T., Fleischhacker, A., Grube, M. & Muggia, L. 2017. ITS1 metabarcoding highlights low specificity of lichen mycobiomes at a local scale. *Mol. Ecol.* 26:4811–30.

Gardes, M. & Bruns, T. D. 1993. ITS primers with enhanced specificity for basidiomycetes application to the identification of mycorrhizae and rusts. *Mol. Ecol.* 2:113–8.

Grube, M., Cardinale, M., de Castro, J. V., Müller, H. & Berg, G. 2009. Species-specific structural and functional diversity of bacterial communities in lichen symbioses. *ISME J.* 3:1105.

Grube, M., Cernava, T., Soh, J., Fuchs, S., Aschenbrenner, I., Lassek, C., Wegner, U., Becher, D., Riedel, K., Sensen, C. W. & Berg, G. 2015. Exploring functional contexts of symbiotic sustain within lichen-associated bacteria by comparative omics. *ISME J.* 9:412–24.

Gueidan, C., Elix, J. A., McCarthy, P. M., Roux, C., Mallen-Cooper, M. & Kantvilas, G. 2019. PacBio amplicon sequencing for metabarcoding of mixed DNA samples from lichen herbarium specimens. *Mycokeys* 53:73.

Hawksworth, D. L. & Grube, M. 2020. Lichens redefined as complex ecosystems. *New Phytol.* 227:1281–3.

Helms, G., Friedl, T., Rambold, G. & Mayrhofer, H. 2001. Identification of photobionts from the lichen family Physciaceae using algal-specific ITS rDNA sequencing. *Lichenologist* 33:73–86.

Honneger, R. 1992. Lichens: mycobiont-photobiont relationships. *In* Reisser, W. [Ed.] *Algae and Symbioses*. Biopress, Bristol, pp 255–75.

Katoh, K., Misawa, K., Kuma, K. & Miyata, T. 2002. MAFFT: a novel method for rapid multiple sequence alignment based on fast Fourier transform. *Nucleic Acids Res.* 30:3059–66.

Katoh, K. & Toh, H. 2008. Recent developments in the MAFFT multiple sequencealignment program. *Brief. Bioinform.* 9:286–98.

Kirk, P. M., Cannon, P. F., David, J. C. & Stalpers, J. 2001. *Ainsworth and Bisby's Dictionary of the Fungi*, 9th edn. CAB International, Wllingford, 655 pp.

Leavitt, S. D., Kraichak, E., Nelsen, M. P., Altermann, S., Divakar, P. K., Alors, D., Esslinger, T. L., Crespo, A. & Lumbsch, T. 2015. Fungal specificity and selectivity for algae play a major role in determining lichen partnerships across diverse ecogeographic regions in the lichen-forming family Parmeliaceae (Ascomycota). *Mol. Ecol.* 24:3779–97.

Leavitt, S. D., Kraichak, E., Vondrak, J., Nelsen, M. P., Sohrabi, M., Pérez-Ortega, S., St Clair, L. L. & Lumbsch, T. 2016. Cryptic diversity and symbiont interactions in rock-posy lichens. *Mol. Phylogenet. Evol.* 99:261–74.

Leavitt, S. D., Nelsen, M. P., Lumbsch, H. T., Johnson, L. A. & St Clair, L. L.2013. Symbiont flexibility in subalpine rock shield lichen communities in the southwestern USA. *Bryologist* 116:149–61.

Leigh, J. W. & Bryant, D. 2015. POPART: full-feature software for haplotype network construction. *Methods Ecol. Evol.* 6:1110–6.

Lücking, R., Hodkinson, B. P. & Leavitt, S. D. 2016. The 2016 classification of lichenized fungi in the Ascomycota and Basidiomycota – approaching one thousand genera. *Bryologist* 119:361–416.

Marini, L., Nascimbene, J. & Nimis, P. L. 2011. Large-scale patterns of epiphytic lichen species richness: photobiont-dependent response to climate and forest structure. *Sci. Total Environ.* 409:4381–6.

Mark, K., Cornejo, C., Keller, C., Flück, D. & Scheidegger, C. 2016. Barcoding lichen-forming fungi using 454 pyrosequencing is challenged by artifactual and biological sequence variation. *Genome* 59:685–704.

Miller, M. A., Pfeiffer, W. & Schwartz, T. 2010. Creating the CIPRES Science Gateway for inference of large phylogenetic trees. *In Proceedings of the Gateway Computing Environments Workshop. New Orleans, LA, USA* (pp. 1–8).

Molins, A., Moya, P., García-Breijo, F., Reig-Armiñana, J. & Barreno, E. 2018. Assessing lichen microalgal diversity by a

multi-tool approach: isolation, Sanger sequencing, HTS and ultrastructural correlations. *Lichenologist* 50:123–38.
Moya, P., Molins, A., Martínez-Alberola, F., Muggia, L. & Barreno, E. 2017. Unexpected associated microalgal diversity in the lichen *Ramalina farinacea* is uncovered by pyrosequencing analyses. *PLoS ONE* 12:e0175091.
Muggia, L. & Grube, M. 2018. Fungal diversity in lichens: from extremotolerance to interactions with algae. *Life* 8:15.
Muggia, L., Leavitt, S. & Barreno, E. 2018. The hidden diversity of lichenised Trebouxiophyceae (Chlorophyta). *Phycologia* 57:503–24.
Muggia, L., Nelsen, M., Kirika, P. M., Barreno, E., Beck, A., Lindgren, H., Lumbsch, H. T., Leavitt, S. D. & Trebouxia working group. 2020. A phylogenetic overview on the diversity of the predominant lichen photobiont genus *Trebouxia* (Trebouxiophyceae, Chlorophyta). *Mol. Phyl. Evol.* 149:106821.
Muggia, L., Pérez-Ortega, S., Kopun, T., Zellnig, G. & Grube, M. 2014. Phycobiont selectivity leads to ecological tolerance and evolutionary divergence in a polymorphic complex of lichenized fungi. *Ann. Bot.* 114:463–75.
Muggia, L., Zellnig, G., Rabensteiner, J. & Grube, M. 2010. Morphological and phylogenetic study of algal partners associated with the lichen-forming fungus *Tephromela atra* from the Mediterranean region. *Symbiosis* 51:149–60.
Nilsson, R. H., Larsson, K. H., Taylor, A. F. S., Bengtsson-Palme, J., Jeppesen, T. S., Schigel, D., Kennedy, P. et al. 2018. The UNITE database for molecular identification of fungi: handling dark taxa and parallel taxonomic classifications. *Nucleic Acids Res.* 47:259–64.
Nyati, S., Bhattacharya, D., Werth, S. & Honegger, R. 2013. Phylogenetic analysis of LSU and SSU rDNA group I introns of lichen photobionts associated with the genera *Xanthoria* and *Xanthomendoza* (Teloschistaceae, lichenized Ascomycetes). *J. Phycol.* 49:1154–66.
Onuț-Brännström, I., Benjamin, M., Scofield, D. G., Heiðmarsson, S., Andersson, M. G., Lindström, E. S. & Johannensson, H. 2018. Sharing of photobionts in sympatric populations of *Thamnolia* and *Cetraria* lichens: evidence from high-throughput sequencing. *Sci. Rep.* 8:4406.
Paul, F., Otte, J., Schmitt, I. & Dal Grande, F. 2018. Comparing sanger sequencing and high-throughput metabarcoding for inferring photobiont diversity in lichens. *Sci. Rep.* 8:8624.
Paulson, J. N., Stine, O. C., Bravo, H. C. & Pop, M. 2013. Differential abundance analysis for microbial marker-gene surveys. *Nat. Methods* 10:1200–2.
Peksa, O. & Škaloud, P. 2011. Do photobionts influence the ecology of lichens? A case study of environmental preferences in symbiotic green alga *Asterochloris* (Trebouxiophyceae). *Mol. Ecol.* 20:3936–48.
Piercey-Normore, M. D. & DePriest, P. T. 2001. Algal switching among lichen symbioses. *Am. J. Bot.* 88:1490–8.
Quast, C., Pruesse, E., Yilmaz, P., Gerken, J., Schweer, T., Yarza, P., Peplies, J. & Glöckner, F. O. 2013. The SILVA ribosomal RNA gene database project: improved data processing and web-based tolos. *Nucleic Acids Res.* 41:D590–6.
Rambold, G., Friedl, T. & Beck, A. 1998. Photobionts in lichens: possible indicators of phylogenetic relationships. *Bryologist* 101:92–397.
Romeike, J., Friedl, T., Helms, G. & Ott, S. 2002. Genetic diversity of algal and fungal partners in our pecies of *Umbilicaria* (Lichenized Ascomycetes) Along a Transect of the Antarctic Peninsula. *Mol. Biol. Evol.* 19:1209–17.
Ronquist, F., Teslenko, M., van der Mark, P., Ayres, D. L., Darling, A., Höhna, S., Larget, B., Liu, L., Suchard, M. A. & Huelsenbeck, J. P. 2012. MrBayes 3.2: efficient Bayesian phylogenetic inference and model choice across a large model space. *Systems Biol.* 61:539–42.
Singh, G., Dal Grande, F., Divakar, P. K., Otte, J., Crespo, A. & Schmitt, I. 2017. Fungal-algal association patterns in lichen symbiosis linked to microclimate. *New Phytol.* 214:317–29.
Smith, H. B., Dal Grande, F., Muggia, L., Keuler, R., Divakar, P. K., Grewe, F., Schmitt, I., Lumbsch, H. T. & Leavitt, S. D. 2020. Metagenomic data reveal diverse fungal and algal communities associated with the lichen symbiosis. *Symbiosis* 82(1-2):133–147.
Spribille, T. 2018. Relative symbiont input and the lichen symbiotic outcome. *Curr. Opin. Plant Biol.* 44:57–63.
Spribille, T., Tagirdzhanova, G., Goyette, S., Tuovinen, V., Case, R. & Zandberg, W. F. 2020. 3D biofilms: in search of the polysaccharides holding together lichen symbioses. *FEMS Microbiol. Letters* 367:fnaa023.
Stamatakis, A. 2006. RAxML-VI-HPC: maximum likelihood-based phylogenetic analyses with thousands of taxa and mixed models. *Bioinformatics* 22:2688–90.
Stamatakis, A., Hoover, P. & Rougemont, J. 2008. A rapid bootstrap algorithm for the RAxML web servers. *Syst. Biol.* 57:758–71.
Steinová, J., Škaloud, P., Yahr, R., Bestová, H. & Muggia, L. 2019. Reproductive and dispersal strategies shape the diversity of mycobiont-photobiont association in *Cladonia* lichens. *Mol. Phylogenet Evol.* 134:226–37.
U'Ren, J. M., Lutzoni, F., Miadlikowska, J., Zimmerman, N. B., Carbone, I., May, G. & Arnold, A. E. 2019. Host availability drives distributions of fungal endophytes in the imperilled boreal realm. *Nat. Ecol. Evol.* 3:1430–7.
U'Ren, J. M., Riddle, J. M., Monacell, J. T., Carbone, I., Miadlikowska, J. & Arnold, A. E. 2014. Tissue storage and primer selection influence pyrosequencing-based inferences of diversity and community composition of endolichenic and endophytic fungi. *Mol. Ecol. Res.* 14:1032–48.
Vančurová, L., Muggia, L., Peksa, O., Řídká, T. & Škaloud, P. 2018. The complexity of symbiotic interactions influences the ecological amplitude of the host: a case study in *Stereocaulon* (lichenized ascomycota). *Mol. Ecol.* 27:3016–33.
Voytsekhovich, A. & Beck, A. 2016. Lichen photobionts of the rocky outcrops of Karadag massif (Crimean Peninsula). *Symbiosis* 68:9–24.
White, T. J., Burns, T., Lee, S. & Taylor, J. 1990. *Amplification and Direct Sequencing of Fungal Ribosomal DNA Genes for Phylogenetics.* Academics Press, Florida, pp 315–322.
Xu, M., De Boer, H., Olafsdottir, E. S., Omarsdottir, S. & Heidmarsson, S. 2020. Phylogenetic diversity of the lichenized algal genus *Trebouxia* (Trebouxiophyceae, Chlorophyta): a new lineage and novel insights from fungal-algal association patterns of Icelandic cetrarioid lichens (Parmeliaceae, Ascomycota). *Bot. J. Linn. Soc.* 194:460–8.
Yahr, R., Vilgalys, R. & Depriest, P. T. 2004. Strong fungal specificity and selectivity for algal symbionts in Florida scrub *Cladonia* lichens. *Mol. Ecol.* 13:3367–78.
Yahr, R., Vilgalys, R. & Depriest, P. T. 2006. Geographic variation in algal partners of *Cladonia subtenuis* (Cladoniaceae) highlights the dynamic nature of a lichen symbiosis. *New Phytol.* 171:847–860.

Supporting Information

Additional Supporting Information may be found in the online version of this article at the publisher's web site:

Figure S1. Haplotype networks based on nrITS of the mycobiont *Ramalina farinacea*. Each circle represents a haplotype, the size of each circle is proportional to the number of individuals sharing that haplotype. Lines between circles represent mutational steps. The geographical origin of the individuals is color-coded as follows: orange—Azuébar, green—Montaña Quemada, pink—San Isidro, dark green—Pista Ovejeros and blue—San José de los Llanos. Specimens representing each haplotype are listed in the table on the right.

Figure S2. Phylogenetic analysis of *Trebouxia* species found in thalli of *Ramalina farinacea*. The analyses are based on the ITS1-5.8S gene fragments of 128 ASVs of *Trebouxia*, 26 representatives of well-accepted species from the SAG and UTEX, *Trebouxia* sp. TR9, *T. crespoana* and 10 OTUs described by Leavitt et al. (2015) and Moya et al. (2017) retrieved from GenBank. Twelve sequences obtained by blast search against whole GenBank database for each ASV. The four principal lineages recognized in *Trebouxia* are recognized according Helms (2002) and Muggia et al. (2020), that is, clade A, C, I and S. *Trebouxia* spp. detected in the assay are highlighted in grey. Values at nodes indicate bootstrap support (RAxML analysis) and posterior probability values (Bayesian analysis). Scale bar shows the estimated number of substitutions per site.

Figure S3. Graphs of mean relative abundance of *Trebouxia* species for all the samples found in (A) Iberian Peninsula, (B) Tenerife and (C) La Palma.

Figure S4. Principal coordinates analysis (PCoA) based on Bray-Curtis (A) for samples from all the five localities treated as pooled AMB collected from the tree 1 ($n = 30$) colour-coded by branch, and (B, C) for samples treated as AMB considering all five trees branch 1 ($n = 15$) colour-coded by tree (B), Azuébar and (C), San Isidro.

Table S1. Per sample locality, tree, branch, part, size and reads number.

Table S2. ASVs abundances per sample present with more than 1000 reads in the entire data set and taxonomic assignment of each ASV.

Table S3. ASVs abundances per region. (A) *Trebouxia* spp.; (B) *Asterochloris* sp.; (C) Other algae and (D) No significant similarity found.

Table S4. Pairwise Kruskal–Wallis tests for alpha diversity differences among thallus size and thallus parts. (A) Shannon Index (pairwise Kruskal-Wallis test) **P*-values < 0.05. (B) Evenness Index (pairwise Kruskal-Wallis test) **P*-values < 0.05. (C) Faith pd (pairwise Kruskal-Wallis test).

Table S5. Pairwise PERMANOVA tests for beta diversity differences among branches 1 and 2 from tree 1 and trees. (A) Bray Curtis by branch for the five localities Pairwise PERMONAVA results. (B) By tree Azuébar. Pairwise PERMONAVA results. (C) By tree San Isidro. Pairwise PERMONAVA results.

Table S6. Pairwise PERMANOVA tests for beta diversity differences among region. (A) Bray Curtis Pairwise PERMONAVA results **P*-values < 0.05. (B) Unweighted Pairwise PERMONAVA results **P*-values < 0.05. (C) Weighted Pairwise PERMONAVA results **P*-values < 0.05.